Algorithms for Constructing 3-D Point Clouds Using Multiple Digital Fringe Projection Patterns

Tao Peng[1], Satyandra K. Gupta[2] and Kam Lau[3]

[1]University of Maryland at College Park, pengtao@eng.umd.edu
[2]University of Maryland at College Park, skgupta@eng.umd.edu
[3]Automated Precision Inc., kam.lau@apisensor.com

ABSTRACT

This paper describes algorithms for generating 3-D point clouds from a set of digital images obtained from projecting phase-shifted sinusoidal fringe patterns onto object. In this paper, a mathematical model is introduced for describing the geometric relationship between the fringe patterns being projected, the image captured and the shape of the object being measured. This model allows considerable flexibility in the spatial configuration of shape measurement system. The algorithms for point cloud construction described in this paper present an improvement over the existing algorithms in terms of accuracy, ease of system calibration, and sensitivity to parameter errors. These algorithms have been incorporated in a shape measurement system and shown to have a very good performance.

Keywords: 3-D shape measurement, fringe projection, point cloud generation, triangulation.

1. INTRODUCTION

Many industrial applications require accurate and rapid measurement of the 3-D shapes of objects. Representative applications of 3-D shape measurement include reverse engineering, 3D replication, inspection and quality control. In most of these applications, users need to construct 3D point clouds that correspond to the objects surface by performing measurement on the objects surfaces. Manufacturing industry needs a fast inspection process that can measure and analyze various 3D features on the part and determine if a feature is within the tolerance specifications or not. The measurement scheme needs to be adequately accurate to eliminate measurement errors. Measurement errors can lead to erroneous inspection that results in an acceptable part being rejected and a defective part being accepted. Hence, both inspection speed and accuracy are equally important.

Coordinate measurement machines and laser based measurement techniques usually provide very accurate measurements. However, these techniques are slow because they measure various points on the part sequentially. On the other hand, camera-based techniques are usually very fast. Therefore, a possible way to perform the 3D inspection is to use digital cameras to construct a dense point cloud (e.g., points spaced less then 0.25mm apart) corresponding to the part being inspected and then analyze the point cloud to determine if it meets the tolerance specifications. But accuracy associated with the conventional camera-based inspection techniques has not been very high in the area of measurement of geometrically complex 3D shapes.

Shape measurement based on digital fringe projection (SMDFP) is a technique for non-contact shape measurement. Due to its fast speed, flexibility, low cost and potentially high accuracy, SMDFP has shown great promise in 3-D shape measurement, especially for applications that require acquisition of dense point clouds. A typical SMDFP system contains one projection unit and one or more cameras (a schematic of a SMDFP system with one projector and one camera is shown in Fig. 1). During the shape measurement process, a set of fringe patterns, whose structures are accurately controlled by computer, are projected onto the surface of the object being measured. Meanwhile, the images of the object shone by the light patterns are captured by the digital camera(s). By using image processing techniques and the triangulation method, a dense 3-D point cloud representing the surface of the object can be constructed.

From the view of mathematical model, existing SMDFP systems can be put into two categories, calibration matrix based models and optical geometry based models [2]. For the calibration matrix based models [3], the whole measurement volume of the system needs to be calibrated by measuring a special calibration plate at a number of different positions (typically over 12), and as a result a huge 3-D coefficient matrix is generated. Based on this matrix,

the construction of the point cloud (representing the object's surface) is done by means of polynomial interpolations. There are two major disadvantages of this approach. One is the truncation error caused by presenting the measurement volume using discrete (calibration) nodes and polynomials with limited order. The second is the time-consuming calibration procedure and re-calibrations. Each time the system's optical setup is changed, no matter how minor it is, the complete calibration has to be redone. For optical geometry based models [4][5], the computation of point cloud is based on a geometric model of the SMDFP system and associated parameters, which could describe the measurement volume very accurately if every single element of the optical geometry is modeled appropriately. Unlike the calibration matrix, the optical geometry based model describes individual system components in separate groups of parameters. If the system configuration is changed partly, only a limited number of geometric parameters will be affected and hence can be measured or estimated specifically, which simplifies the re-calibration and saves time. However, due to the complexity of the optical geometry of SMDFP system, existing models make inaccurate assumptions or ignore some minor parameters for simplification [5], which makes the system less accurate and less flexible in terms of spatial configurations.

In this paper, a comprehensive mathematical model for SMDFP system is introduced, which models the optical geometry of SMDFP system accurately. By utilizing this mathematical model, a new algorithm for point cloud construction is developed, which ensures the accuracy, flexibility and ease of calibration of the system. Improvements made on other algorithms involved in shape reconstruction are also described.

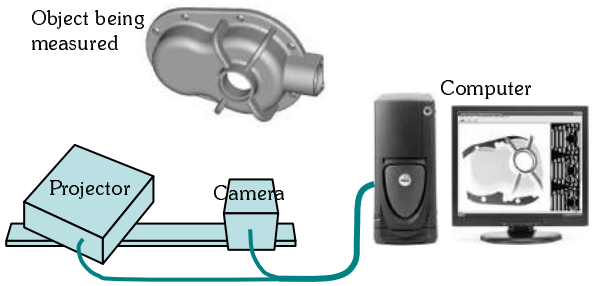

Fig. 1. Schematic of a SMDFP system with one projector and one camera.

2. OVERVIEW OF APPROACH

The SMDFP system utilized in our research uses a digital micro-mirror device (DMD) to generate a projection pattern and digital camera to take the images. This system generates an appropriate projection pattern and uses a DMD-based projection unit to project the pattern on the object being measured. The digital camera takes images of the object. Due to three-dimensional nature of the object surface, the projected pattern distorts. The images captured by camera records the distortion in the projection pattern. Images captured by the camera are analyzed by the system to estimate the 3D points on the object surface that cause the distortion in the projection pattern seen in the image. The system finally returns a 3D point cloud that represents the object surface.

One of the key features behind the new system is use multiple projection patterns. Different projection patterns lead to different accuracy. A projection pattern that produces accurate result for one shape feature may not be ideal for some other feature. Hence, different projection patterns are needed to capture different features on the object accurately. The use of multiple projection patterns allows the system to measure all the features on the object accurately. The system also selects the projection patterns carefully to minimize the number of patterns being used to keep the measurement process fast. Another novel feature of the system is use of a high fidelity mathematical model for every element of the system. This helps in improving the overall measurement accuracy. A detailed description of the proposed mathematical model for SMDFP system is given in Sec. 3.

Based on this model, the shape measurement process and the relationship of the algorithms involved in shape reconstruction can be depicted by Fig. 2. Below is a short description for each individual step:

- **Algorithm for construction of absolute phase map**: In a shape measurement procedure, a set of phase-shifted sinusoidal fringe patterns, which are generated by the *phase-shifting algorithm*, are projected onto the surface of the object being measured. The images of the object, under the illumination of the patterns, are captured by the camera. These images are processed by the phase recovery and phase unwrapping algorithm and the outcome is an absolute phase map of the object, which is a 2-D matrix with the same dimension as the raw image and each element in the matrix is a phase value (real number) that

corresponds to a point on the object's surface. The combination of phase-shifting algorithm, phase recovery and phase unwrapping algorithm is called the *algorithm for phase map construction* (see Sec. 4 for details).

- **Algorithm for construction of point cloud**: The *point cloud construction algorithm* is built on top of the optical geometry model of the system. It converts the absolute phase map of the object into a dense 3-D point cloud that represents the surface of the object (see Sec. 5 for details).
- **Algorithm for estimation of parameters**: As mentioned above, the optical geometry model consists of a number of geometric parameters (also called sensor parameters). The role of *parameter estimation algorithm* is to accurately evaluate these parameters, since most of them involve optical characteristics and therefore cannot be measured directly. Tailored for the support of the proposed mathematical model, the parameter estimation algorithm we used can be divided into two parts, camera calibration algorithm [8][9] and the estimation of the projection center's position for the projector. We use algorithms described in Ref. [9] for camera calibration and developed a new algorithm for estimating the projection center's position for the projector.

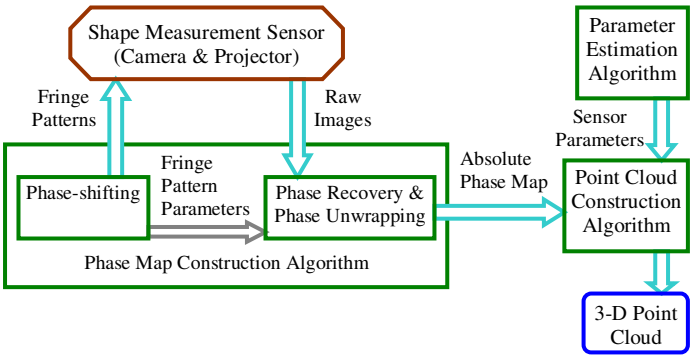

Fig. 2. Relationship of the algorithms involved in shape reconstruction.

3. MATHEMATICAL MODEL

3.1 Central Projection Model for the Camera

The central projection model, a.k.a. pinhole camera model, has been shown to be an accurate mathematical model for cameras. It is widely used in areas such as photogrammetry, machine vision and computer graphics. A complete central projection model with lens distortion consideration can be described by a series of transformations as follows (see Fig. 3):

1. **Transformation from the world coordinate to the camera coordinate**: In the central projection model, each camera defines a camera coordinate frame (Cartesian), which is determined by the camera's optics and image formation hardware, e.g. the CCD. The coordinate transformation between the world coordinate frame and the camera coordinate frame can be described by a rotation matrix $\mathbf{R}_{W2C}$ and a translation vector $\mathbf{T}_{W2C}$:

$$\left[x_M^{(C)}, y_M^{(C)}, z_M^{(C)}\right]^T = \mathbf{R}_{W2C} \cdot \left[x_M^{(W)}, y_M^{(W)}, z_M^{(W)}\right]^T + \mathbf{T}_{W2C} \quad (1)$$

where $\left[x_M^{(W)}, y_M^{(W)}, z_M^{(W)}\right]^T$ is the coordinates of point M in the world coordinate frame and $\left[x_M^{(C)}, y_M^{(C)}, z_M^{(C)}\right]^T$ is the coordinates of point M in the camera coordinate frame.

2. **Perspective projection to the image plane**: As a convention, the image plane of the central projection is defined as the plane perpendicular to $Z^{(C)}$ axis and intersecting it at $z^{(C)} = -1$. The two axes of the image plane, $\mathbf{u}$ and $\mathbf{v}$, are parallel to $X^{(C)}$ and $Y^{(C)}$ axis respectively. The principle point of the central projection is defined as the intersection of $Z^{(C)}$ axis with the image plane, whose pixel coordinates are

(u_0, v_0). Let M_I denote the projection of point M on the image plane. The coordinates of M_I in the camera coordinate frame, that is $\left[x_M^{(n)}, y_M^{(n)}, -1\right]^T$, are calculated as follows:

$$\left[x_M^{(n)}, y_M^{(n)}, -1\right]^T = \left[\frac{x_M^{(C)}}{-z_M^{(C)}}, \frac{y_M^{(C)}}{-z_M^{(C)}}, \frac{z_M^{(C)}}{-z_M^{(C)}}\right]^T \tag{2}$$

3. **Lens distortion model**: Due to the distortion of optical lenses, the perspective projection is never perfect for a real camera. Therefore, the real position of M_I is usually not the ideal one, that is $\left[x_M^{(n)}, y_M^{(n)}, -1\right]^T$, but it is shifted a little in the $\mathbf{u}-\mathbf{v}$ plane and ends up at $\left[x_M^{(d)}, y_M^{(d)}, -1\right]^T$. The most popularly used lens distortion model in photogrammetry is the one introduced by Brown [6], in which the relationship between the distorted projection position, $\left[x_M^{(d)}, y_M^{(d)}, -1\right]^T$, and the idealized projection position, $\left[x_M^{(n)}, y_M^{(n)}, -1\right]^T$, is defined as follows:

$$\begin{bmatrix} x_M^{|d|} \\ y_M^{|d|} \end{bmatrix} = \left(1 + k_1 r^2 + k_2 r^4 + k_5 r^6\right) \begin{bmatrix} x_M^{|n|} \\ y_M^{|n|} \end{bmatrix} + \begin{bmatrix} 2k_3 x_M^{|n|} y_M^{|n|} + k_4\left(r^2 + 2\left(x_M^{(n)}\right)^2\right) \\ k_3\left(r^2 + 2\left(y_M^{(n)}\right)^2\right) + 2k_4 x_M^{|n|} y_M^{|n|} \end{bmatrix} \tag{3}$$

where $r^2 = \left(x_M^{(n)}\right)^2 + \left(y_M^{(n)}\right)^2$ and k_i ($k = 1, \ldots, 5$) are the radial and tangential distortion coefficients of the lenses.

4. **Transformation from the camera coordinate to the pixel coordinate**: For a digital camera (typically CCD or CMOS based), the position of M_I will be digitized by the CCD/CMOS chip and presented in pixel coordinates eventually. Denote $\left[x_M^{(p)}, y_M^{(p)}, -1\right]^T$ as the homogeneous pixel coordinates for M_I, which can be calculated from the following equation:

$$\begin{bmatrix} x_M^{(p)} \\ y_M^{(p)} \\ 1 \end{bmatrix} = \mathbf{A} \cdot \begin{bmatrix} x_M^{(d)} \\ y_M^{(d)} \\ 1 \end{bmatrix} \quad , \quad \mathbf{A} = \begin{bmatrix} f_x & \alpha f_x & u_0 \\ 0 & f_y & v_0 \\ 0 & 0 & 1 \end{bmatrix} \tag{4}$$

where $\mathbf{A}$ is called the camera's intrinsic matrix, in which (u_0, v_0) is the pixel coordinates of the principle point, f_x and f_y are the scale factors for axes $\mathbf{u}$ and $\mathbf{v}$ respectively, and α is a coefficient describing the skewness of axes $\mathbf{u}$ and $\mathbf{v}$.

5. **Inverse transformations (from the pixel coordinate to the world coordinate)**: Shape reconstruction is a process to calculate the world coordinates of points from image(s). Therefore, the inverse operations of the above procedures are required. We construct this model by computing inverse of the above four transformations.

3.2 Mathematical Model for the Overall System

The proposed mathematical model for SMDFP system can be decomposed into three parts: camera model, projector model and sensor coordinate frame. The camera model used is a central projection model with consideration of lens distortion, as explained in Sec. 3.1. A computer projector (LCD or DMD based) acts as an inverted digital camera from the optical geometry point of view. Therefore, it can also be described accurately by a central projection model as the camera does. As it can be seen in Fig. 4, a Cartesian coordinate frame $X^{(P)}Y^{(P)}Z^{(P)}$ is defined by the projector. The image plane defined by $\xi - \eta$ axes represents the LCD/DMD chip of the projector. The pixel coordinates of the

principle point are (ξ_0, η_0). All the transformations associated with the central projection model are identical to those described for the camera (see Sec. 3.1). The sensor coordinate frame, $X^{(S)}Y^{(S)}Z^{(S)}$, is the coordinate frame with respect to which the camera model and the projector model are defined. In this paper, the projector model and the camera model will be fixed with respect to the world coordinate frame, i.e. there will be no sensor movement. The sensor coordinate frame is defined as coinciding with the world coordinate frame for the sake of convenience.

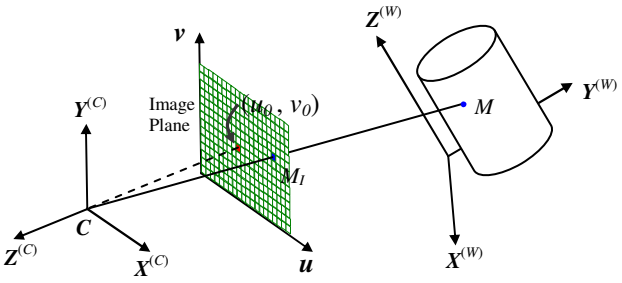

Fig. 3. Central projection model for the camera.

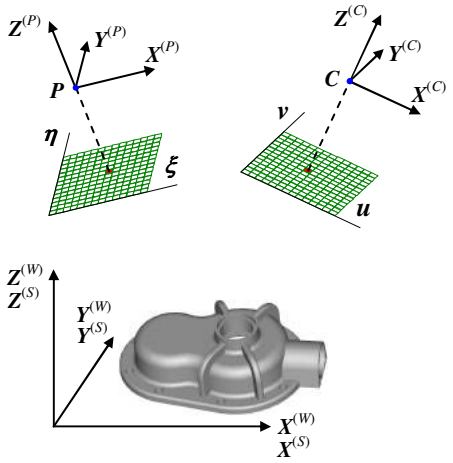

Fig. 4. Mathematical model for the overall system.

4. ALGORITHM FOR CONSTRUCTION OF ABSOLUTE PHASE MAP

The functionality of phase map construction algorithm is to generate an absolute phase map from a set of images obtained from phase-shifting technique. Among the numerous existing algorithms, phase-shifting with multiple fringe frequencies appears to be a very promising method for shape measurement of objects with complex shapes [7]. Here, we propose a phase map construction algorithm that is based on the conventional phase-shifting with multiple fringe frequencies but uses fewer fringe patterns.

Taking the phase map construction algorithm with 4-step phase-shifting and 3 fringe frequencies as an example, it requires a total of 12 phase-shifted sinusoidal fringe patterns, which can be defined by the following equations:

$$I_n^{(P),k}(\xi,\eta) = \frac{I_{\max}^{(P)}}{2}\left[1+\sin\left(c_k \cdot \xi + \frac{n\cdot\pi}{2}\right)\right] \tag{5}$$

where $k = 0,1,2$ represents different fringe frequencies;

$n = 1,\ldots,4$ represents different phase-shift value;

c_k is a coefficient indicating the fringe frequency of a pattern (number of fringes in a pattern);

$I_{\max}^{(P)}$ is the maximum intensity (brightness) of the pattern; and

$I_n^{(P),k}(\xi,\eta)$ is the intensity of each pixel in the fringe pattern defined in the $\xi-\eta$ plane of the projector.

Using the 12 fringe patterns for projection, the corresponding images of the object under projection can be described by the following equations:

$$I_n^{(k)}(i,j) = A(i,j) + B(i,j)\sin\left[\Phi^{(k)}(i,j) + \frac{n\cdot\pi}{2}\right] \tag{6}$$

where $k = 0,1,2$ represents different fringe frequencies, $n = 1,\ldots,4$ represents different phase-shift value and (i,j) are indices for pixels in the image. For each pixel (i,j), $A(i,j)$ and $B(i,j)$ are constants, $\Phi^{(k)}(i,j)$ is the associated

absolute phase value, and $I_n^{(k)}(i,j)$ is the pixel's grayscale intensity corresponding to the $(k+1)$-th fringe frequency and the n-th phase-shift.

Notice that for each pixel (i,j), $A(i,j)$ and $B(i,j)$ are constants for all the 12 images. Also, $A(i,j)$ and $B(i,j)$ can be evaluated from the set of four images that correspond to the same fringe frequency but with different phase-shift value. Therefore, by taking advantage of the common $A(i,j)$ and $B(i,j)$ that are shared by all the images, the number of fringe patterns required in the phase map construction algorithm can be reduced by using the following approach:

- Firstly, $A(i,j)$ and $B(i,j)$ can be evaluated from one set of images that correspond to the same fringe frequency;
- Secondly, the evaluated $A(i,j)$ and $B(i,j)$ can be applied to the phase recovery of images being obtained from other fringe frequencies. By using $A(i,j)$ and $B(i,j)$ as known, the number of images required for phase recovery can be reduced to 2 or even 1.

Applying this idea to the phase map construction algorithm with 3 fringe frequencies and 4-step phase-shifting (as described above), the number of fringe patterns required can be reduced to 8. That is, for the fringe patterns defined by Eqn. (5), the patterns corresponding to "($k=0$ or 1) and ($n=3$ or 4)" can be eliminated. The 8 images obtained from the projection of these patterns are then:

$$\begin{aligned} I_1^{(k)}(i,j) &= A(i,j) + B(i,j)\sin\left[\Phi^{(k)}(i,j)+\pi\right] \\ I_2^{(k)}(i,j) &= A(i,j) + B(i,j)\sin\left[\Phi^{(k)}(i,j)+\pi/2\right] \end{aligned} \quad , \quad k=0,1 \tag{7}$$

and

$$I_n^{(2)}(i,j) = A(i,j) + B(i,j)\sin\left[\Phi^{(2)}(i,j)+\frac{n\cdot\pi}{2}\right] \quad , \quad n=1,\ldots,4 \tag{8}$$

The corresponding phase recovery algorithm, which calculates the wrapped phase maps $\phi^{(k)}(i,j)$ ($k=0,1,2$) from the images, needs to be modified as following:

- First, phase map $\phi^{(2)}$ can be computed from the classical equation for 4-step phase shifting:

$$\phi^{(2)}(i,j) = \arctan\left(\frac{I_1^{(2)}(i,j)-I_3^{(2)}(i,j)}{I_2^{(2)}(i,j)-I_4^{(2)}(i,j)}\right) \tag{9}$$

  The coefficients $A(i,j)$ are obtained by solving the Equation set (8).
- Using the values of $A(i,j)$, the phase map $\phi^{(0)}(i,j)$ and $\phi^{(1)}(i,j)$ are computed using the Equation set (7).

Our phase unwrapping algorithm, which computes the absolute phase map $\Phi(i,j)$ from the wrapped phase maps $\phi^{(k)}(i,j)$, is a minor modification of existing algorithms. Hence it will not be discussed here.

This method for elimination of redundant projection patterns can be applied to phase map construction algorithms with any number of fringe frequencies (>1) and any steps of phase-shifting.

5. ALGORITHM FOR CONSTRUCTION OF POINT CLOUD

The point cloud construction algorithm proposed here requires the following information to be known prior to shape reconstruction:

- All extrinsic and intrinsic parameters of the camera, i.e. the rotation matrix $\mathbf{R}_{W2C}$, the translation vector $\mathbf{T}_{W2C}$ with respect to the user-defined world coordinate frame, the intrinsic matrix $\mathbf{A}$ and the lens distortion coefficients k_i ($k=1,\ldots,5$).
- The projection center P for the projector in the world coordinate frame, i.e. $P(P_x,P_y,P_z)$.

- An absolute phase map $\Phi_R(u,v)$ of the XY plane in the world coordinate frame, where u and v are the pixel coordinates in the image.

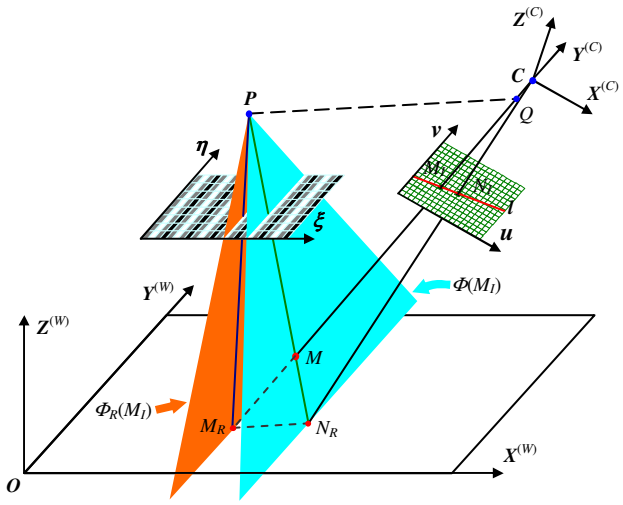

Fig. 5. Triangulation with a reference plane.

In a shape measurement procedure, an absolute phase map, $\Phi_R(u,v)$, of the object being measured is first obtained by the phase map construction algorithm. For any pixel (u,v) in the phase map, the corresponding idealized position on the image plane, M_I, can be calculated from the camera's intrinsic and extrinsic parameters. In this section, all spatial coordinates are in world coordinate frame if not otherwise stated. Assume $M(M_x, M_y, M_z)$ is the point on the object's surface that corresponds to the pixel (u,v), therefore M is on the line $\overline{CM_I}$. Denote M_R as the intersection point of line $\overline{CM_I}$ with the XY plane. Similarly, N_R is the intersection of line $\overline{PM}$ with the XY plane, and N_I is the intersection of line $\overline{CN_R}$ with the image plane. Furthermore, define point Q as the intersection of line $\overline{CM_I}$ with the plane $\mathbf{E}$ (not drawn in Fig. 5), which is parallel to the XY plane and passes through point P. From the definitions of these points, it can be seen that points C, P, Q, M_I, N_I, M_R, N_R and M are all in the same plane, say plane $\mathbf{F}$, and line $\overline{PQ}$ and line $\overline{M_RN_R}$ are parallel to each other, since they are the intersections of plane $\mathbf{F}$ with the XY plane and plane $\mathbf{E}$ respectively. Therefore, from the geometric relationship between the similar triangles ΔMPQ and ΔMN_RM_R, the Z-coordinate M_z of point M can be expressed as a function of $\left|\overline{PQ}\right|$, $\left|\overrightarrow{M_RN_R}\right|$ and P_z, where $\left|\overline{PQ}\right|$ is the length of line $\overline{PQ}$ and $\left|\overrightarrow{M_RN_R}\right|$ is the signed length of line $\overline{M_RN_R}$, i.e.

$$\left|\overrightarrow{M_RN_R}\right| = \left|\overline{M_RN_R}\right| \cdot sign\left(\overrightarrow{PQ} \cdot \overrightarrow{M_RN_R}\right) \tag{10}$$

Among the variables that determine M_z, the only variable left unknown is $\left|\overrightarrow{M_RN_R}\right|$, because the position of N_R is not known. Recall that N_R is the intersection of line $\overline{PM}$ with the XY plane, therefore $\Phi_R(N_R) = \Phi_R(M)$. On

the other hand, since points P, M and N_R are colinear in the 3-D space, their projection points on the image plane $\mathbf{u}-\mathbf{v}$ are colinear as well, i.e. point P_I, M_I and N_I are on the line $\mathbf{l}$. The position of N_I can then be located by finding a point on line $\overline{P_I M_I}$, whose phase value in $\Phi_R(u,v)$ (absolute phase map of the XY plane) is $\Phi_R(M)$. This is done in the pixel coordinate space of the phase map $\Phi_R(u,v)$ (see Fig. 6). Once the pixel coordinates of N_I is known, its world coordinates can be calculated from the camera model and hence the world coordinates of point N_R from the intersection of line $\overline{CN_I}$ with XY plane. After the position of N_R is known, M_z can be easily obtained. At last, M_x and M_y are calculated from the equation of line $\overline{CM_I}$ and M_z.

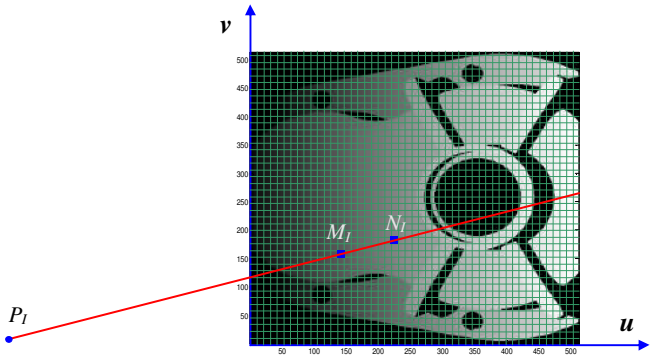

Fig. 6. Find the pixel coordinates of N_I in the phase map of XY plane.

As mentioned in Sec. 1, the mathematical models and associated point cloud construction algorithms for SMDFP system can be divided into two categories [2]: geometric approach and calibration matrix approach. The most recent and advanced mathematical model for geometric approach [4], which is proposed by Legarda-Sáenz et al., adopted the complete central projection model with lens distortion for both the camera and the projector. Therefore the whole system is described by a total number of 32 geometric parameters. No reference phase map or anything else is needed for the computation of point cloud. As for calibration matrix approaches, generally the whole measurement volume will be calibrated and all the information for shape reconstruction is packed into a 3-D matrix with a dimension of $M \times N \times d$, where $M \times N$ is the resolution of the camera and d is the sum of polynomial orders for the interpolation functions. Take Sitnik's algorithm [3] as an example, in which a fifth-order polynomial is used for function $z = Z(\Phi, i, j)$ and two linear functions for $x = X(z, i, j)$ and $y = Y(z, i, j)$ respectively. The sum of polynomial orders is 7 for this particular case.

The point cloud construction algorithm proposed here is a hybrid of the geometric method and the calibration matrix method. For the camera a full central projection model with lens distortion is used. For the projector only the position of projection center, that is $P(P_x, P_y, P_z)$, needs to be known explicitly. The rest of the geometric information is given by the reference phase map in an implicit way. If compared to the purely geometrical approach, this hybrid approach reduces the total number of parameters to about the half. Therefore the algorithm for parameter estimation becomes less complicated and numerically more stable, since there are fewer variables in the nonlinear minimization process. Also the procedure for parameter estimation becomes easier. On the other hand, the hybrid approach doesn't lose any generality or accuracy, for all the geometric parameters are reflected in the model, explicitly or implicitly. If compared to the calibration matrix approach, the hybrid approach is more accurate and at the same time it gets rid of the huge 3-D matrix of polynomial coefficients. It requires only the knowledge of the geometric parameters and an absolute phase map of reference plane to be able to compute the point cloud.

In order to obtain a point cloud that represents the complete surface of the object (i.e., whole-body measurement), the shape measurement sensor has to make multiple measurements of the object from a series of different perspectives. In practice, this is done by either moving the shape measurement device around or rotating the object. Notice that for each measurement, the acquired point cloud is with respect to the local sensor coordinate frame. Therefore, the point clouds have to be transformed to a common world coordinate frame in order to be merged. The transformations are determined by registration of the local sensor coordinate frames in the world coordinate frame, which requires the measurement of the position and orientation of the shape measurement sensor by some means.

6. IMPLEMENTATION AND RESULTS

Based on the proposed mathematical model and algorithms, a computer program was developed for shape reconstruction. A simple shape measurement hardware was also built, which consists of a commercial computer projector (BenQ PB2220, DMD based, 1024×768 resolution, 1700 ANSI lumens) and a B/W digital camera (1/3" Sony CCD, 640 × 480 resolution). Using the developed software and hardware, a number of shape measurement experiments were done on various objects. The shape measurement worked very well with many different kinds of object shapes, despite of surface discontinuities. A measurement accuracy analysis was also conducted by measuring a master gauge with accurately known geometry. The result shows that the developed hardware can reach an average accuracy of 75μm over a measurement volume of 280mm×220mm×250mm, which we believe can still be greatly improved if a more accurate camera calibration procedure has been carried out. Two examples of shape measurements made on a plastic drill housing and an aluminum part are shown in Fig. 7 and Fig. 8 respectively.

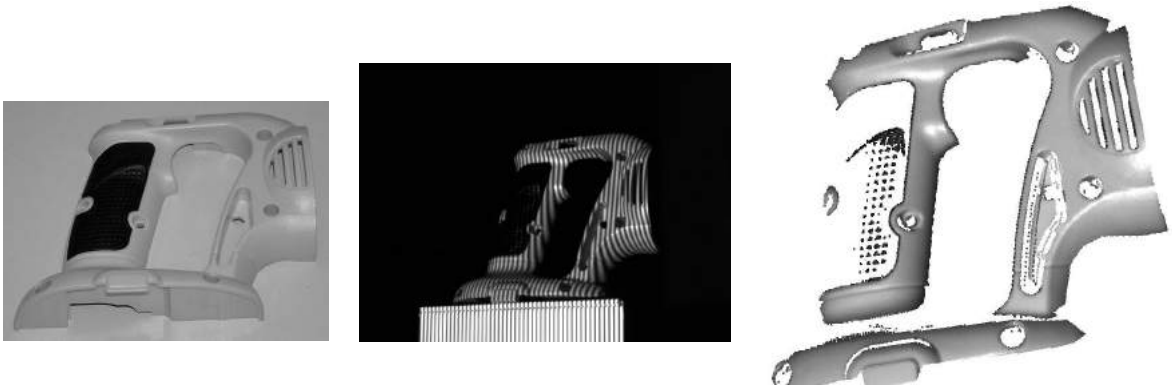

(a). Photograph of the part.

(b). One of the images collected during shape measurement.

(c). Rendering of the dense point cloud that represents the part.

Fig. 7. Generating point clouds for drill housing

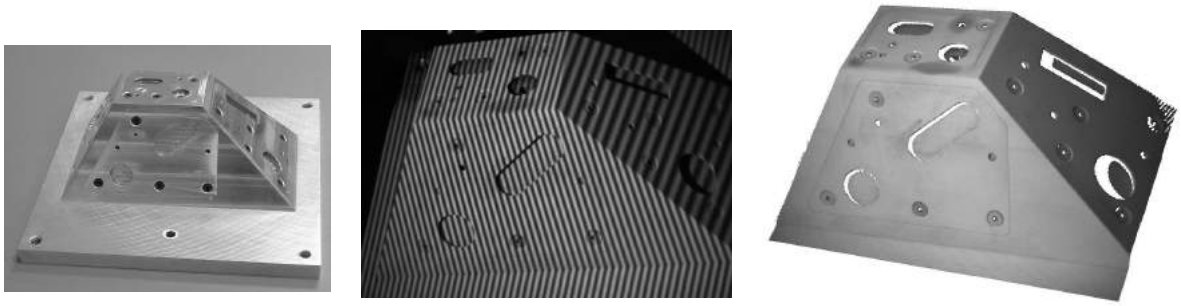

(a). Photograph of the part.

(b). One of the images collected during shape measurement.

(c). Rendering of the dense point cloud that represents the part.

Fig. 8. Generating point clouds for an aluminum part

7. CONCLUSIONS

This paper introduces a comprehensive mathematical model for the SMDFP (Shape Measurement based on Digital Fringe Projection) system, which is a device for generating 3-D point cloud from a set of digital images obtained from projecting phase-shifted sinusoidal fringe patterns onto an object. In addition to the mathematical model, a new algorithm for construction of point cloud is described in the paper. Compared to existing models and algorithms, the proposed mathematical model and point cloud construction algorithm offer a number of advantages, such as better accuracy in shape reconstruction, flexibility in system's spatial configurations and easier calibration of system. An improved algorithm for construction of absolute phase map is also proposed, which uses fewer projection patterns but achieves the same performance as the existing phase-shifting algorithm with multiple fringe frequency. By using fewer projection patterns, the time needed per measurement is reduced. A complete SMDFP system, including software and hardware, has been developed based on the proposed model and algorithms. The system is working very well on a variety of objects with complex shapes. By measuring a master gauge with accurately known geometry, the developed system shows an accuracy of 75μm over a measurement volume of 280mm×220mm×250mm. However, a more accurate calibration procedure for estimation of sensor parameters needs to be developed to fully exploit the high accuracy promised by the proposed model and algorithms.

8. ACKNOWLEDGEMENT

The authors would like to thank Maryland Industrial Partnership program and Automated Precision Inc. for supporting this project.

9. REFERENCES

[1] Chen, F., Brown, G. M. and Song, M., Overview of three-dimensional shape measurement using optical methods, *Optical Engineering*, Vol. 39, No. 1, 2000, pp 10-22.

[2] Breuckmann, B., Halbauer, F., Klaas, E. and Kube, M., 3D-metrologies for industrial applications, *Proceedings of SPIE*, Vol. 3102, 1993, pp 928-930.

[3] Sitnik, R., Kujawińska, M. and Woźnicki, J., Digital fringe projection system for large-volume 360-deg shape measurement, *Optical Engineering*, Vol. 41, No. 2, 2002, pp 443-449.

[4] Legarda-Sáenz, R., Bothe, T. and Jüptner, W. P., Accurate procedure for the calibration of a structured light system, *Optical Engineering*, Vol. 43, No. 2, 2004, pp 464-471.

[5] Hu, Q., Huang, P. S., Fu, Q. and Chiang, F., Calibration of a three-dimensional shape measurement system, *Optical Engineering*, Vol. 42, No. 2, 2003, pp 487-493.

[6] Fryer, J. G. and Brown, D. C., Lens distortion for close-range photogrammetry, *Photogrammetric Engineering and Remote Sensing*, Vol. 52, No. 1, 1986, pp 51-58.

[7] Mermelstein, M. S., Feldkhun, D. L. and Shirley, L. G., Video-rate surface profiling with acousto-optic accordion fringe interferometry, *Optical Engineering*, Vol. 39, No. 1, 2000, pp 106-113.

[8] Salvi, J., Armangué, X. and Batlle, J., A comparative review of camera calibrating methods with accuracy evaluation, *Pattern Recognition*, Vol. 35, No. 7, 2002, pp 1617-1635.

[9] Camera Calibration Toolbox for Matlab, http://www.vision.caltech.edu/bouguetj/calib_doc/.